Polymer 49 (2008) 2217–2222

Contents lists available at ScienceDirect

Polymer

journal homepage: www.elsevier.com/locate/polymer

Formation of polyaniline layer on DNA by electrochemical polymerization

Yosef Bardavid [a], Jamal Ghabboun [a], Danny Porath [a,b], Alexander B. Kotylar [c], Shlomo Yitzchaik [a,b,*]

[a] Institute of Chemistry, The Hebrew University of Jerusalem, Jerusalem 91904, Israel
[b] The Center for Nanoscience and Nanotechnology, The Hebrew University of Jerusalem, Jerusalem 91904, Israel
[c] Department of Biochemistry, George S. Wise Faculty of Life Sciences, Tel Aviv University, Ramat Aviv 69978, Israel

ARTICLE INFO

Article history:
Received 8 November 2007
Received in revised form 5 March 2008
Accepted 6 March 2008
Available online 12 March 2008

Keywords:
Polyaniline
DNA
Nanowires

ABSTRACT

We report the electropolymerization and characterization of polyaniline (PAN) on both DNA monolayer and single poly(dG)–poly(dC) DNA molecules serving as a template. The synthesis includes the formation of an electrostatic complex between the negatively charged DNA and positively charged anilinium ions followed by electrochemical oxidation and polymerization of the anilinium ions' monomers on the DNA template. The polymerization was carried out on a flame annealed gold substrate modified with positively charged self-assembled 4-aminothiophenol (4-ATPh) monolayer. The resulting monolayers and single macromolecular composites of DNA–PAN were characterized by atomic force microscopy (AFM), cyclic voltammetry (CV) impedance and UV–vis spectroscopy.

1. Introduction

Since the discovery of conducting polymers, wide range applications of conducting polymers were suggested [1–3]. Polyaniline (PAN) is one of the most investigated conducting polymers due to the unique properties such as environmental stability, easy proton doping, and versatile redox properties [4,5]. These features are making PAN attractive for different type of electronic applications such as active-sensing layer, electrochromic displays, and electromagnetic shielding [6–8]. However, the obstacles such as poor adhesion on metal substrates and lack of fine control of thickness of the films are the limiting factors for the usage of conductive polymers, producing 2D layers of conducting polymers may overcome these limitations [9,10].

An elegant way for formation of 2D monolayer of PAN on gold and oxide surfaces was showed [11,12] by modifying surfaces with negatively charged monolayers. The strategy applied in these studies is based on electrostatic interaction between the positively charged anilinium monomer and negatively charged SAM layer which yields the formation of anilinium monolayer on the surface and further oxidation of anilinium layer yields the formation of 2D PAN layer on surface. The same electrostatic interaction strategy was applied recently [13] to polyanionic template and formation of 2D PAN layers on poly(styrene-sulfonate) was showed.

DNA is a negatively charged macromolecule due to its phosphate backbone. Besides its biological importance, its unique properties to form complex and pre-designed networks [14,15] makes it attractive as a negatively charged template polymer both for 2D monolayer and single macromolecular wires. Usage of DNA as template for creating conductive nanowires by binding cationic species such as CdS semiconductor nanoparticles [16], silver nanowires [17], gold nanowires [18], and Pd clusters [19] was reported. However, it is difficult to create an electrically continuous chain of nanoparticles because it is likely to have some discontinuity between the metal particles. Additionally, the particles are covered with an insulating organic ligand, leading to poor electronic communication between them or with the DNA [17]. Coating of DNA template by conducting polymers may yield good conducting molecular wires that still preserve the self-assembly properties of the DNA. Conducting polymers' coating of dsDNA bundles or on single DNA molecules using chemical, enzymatic, and photochemical oxidation methods was demonstrated [20,21]. On the other hand electrochemical polymerization has some advantages like control over the final oxidation state of the system, yielding more conducting structures, etc. [22]. To the best of our knowledge, direct *electrochemical oxidation* of anilinium ions aligned on a DNA template was not investigated in details and not shown for single molecules so far. In this study we present a method for formation of PAN layer on stereoregular poly(dG)–poly(dC) dsDNA by electrochemical polymerization. In order to

---

[*] Corresponding author. Institute of Chemistry, The Hebrew University of Jerusalem, Jerusalem 91904, Israel.
E-mail address: sy@cc.huji.ac.il (S. Yitzchaik).

0032-3861/$ – see front matter © 2008 Elsevier Ltd. All rights reserved.
doi:10.1016/j.polymer.2008.03.014

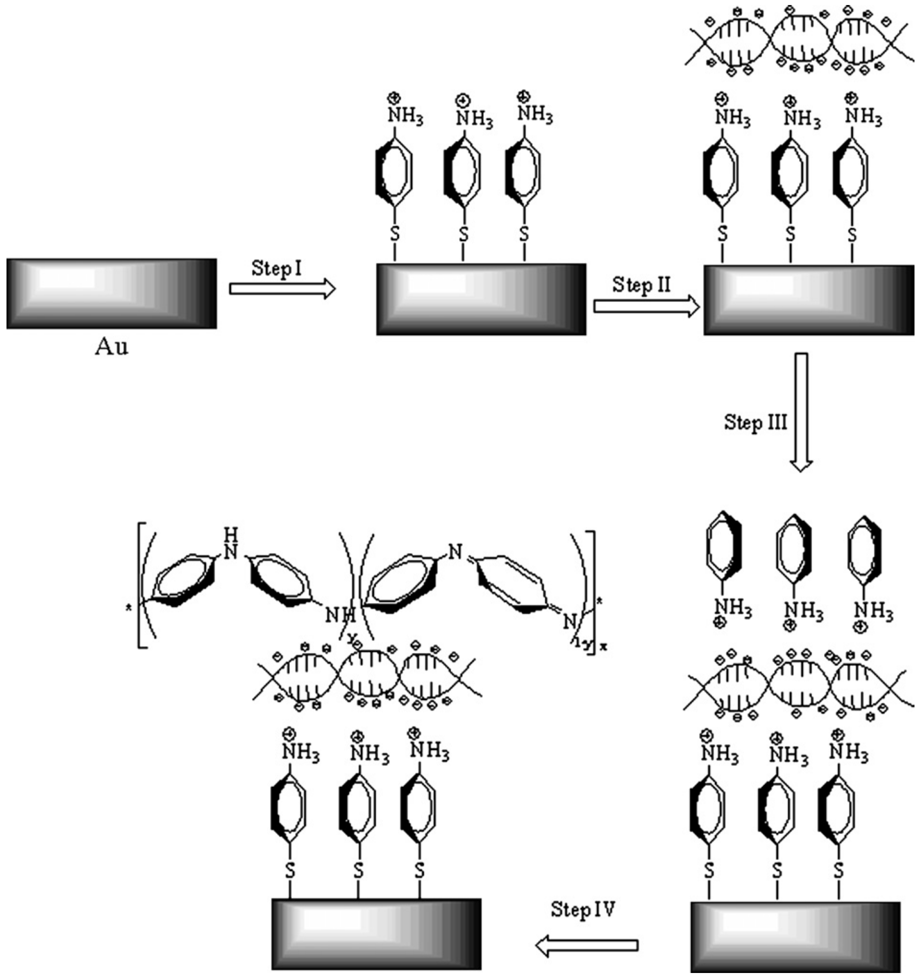

Fig. 1. Synthetic route for wrapping DNA with PAN. The modification of gold with 4-ATPh (step I), DNA immobilization on 4-ATPh modified surface (step II), alignment of anilinium ions on DNA immobilized surface (step III), electropolymerization of anilinium ions (step IV).

immobilize the DNA, a flame annealed gold surface was modified with 4-ATPh [23,24]. The coating of the immobilized DNA was achieved by direct electrochemical oxidation of the anilinium monomers bound to the DNA anchored on a gold surface.

2. Experimental section

Gold surfaces (200 nm thick) on borosilicate (1.1 mm thick) with Cr adhesion layer (2.5 nm) were used as substrates (Arrandee, Germany). The gold substrates were hydrogen flame annealed to achieve highly smooth surfaces with Au(111) terraces of more than $100 \times 100\ \mathrm{nm}^2$ [25]. All the chemicals were used as received except aniline that was freshly distilled prior to usage. The freshly annealed gold was modified with 4-ATPh by immersion in 1 mM ethanol solution of 4-ATPh for 15 h. The treated surface was rinsed with pure ethanol.

The modified surface was incubated with 1–20 nM solution of 2.7 kb poly(dG)–poly(dC) in 20 mM Tris–acetate buffer (pH 7) for 10 min, rinsed with the same buffer, immersed into 1 mM aniline solution (pH 4) for 15 min and further subjected to the electro-oxidative polymerization. Impedance measurements were performed in 5 mM $K_3Fe(CN)_6$ and 0.05 M KCl at a potential of 0.16 V; and an alternating voltage amplitude of 5 mV between 20 KHz and 250 MHz using AUTOLAB PGSTAT12 (Eco Chemie B.V). Electrochemical polymerization of the anilinium ions, bound to the DNA, was carried out with the gold surface as a working electrode, a platinum wire as a counter electrode, and an Ag/AgCl saturated KCl as a reference electrode in 50 mM acetic acid–sodium acetate buffer solution (pH 4) as an electrolyte for electrochemical polymerization.

Absorption spectra were recorded on a Shimadzu UV-310PC scanning spectrophotometer. Atomic force microscopy (AFM) images were acquired in ambient using a Nanotec Electronica S.L system in dynamic mode. Soft, nonconductive, rectangular, commercial SiN cantilevers (OMCL-RC800PSA, Olympus Optical Co., LTD.) with quality factor (Q) $\sim$ 100, spring constant of 0.4–0.8 N m^{-1}, resonance frequency of 75–80 KHz and tip radius of $\sim$15 nm were used. The images were analyzed with the WSxM software [26].

3. Results and discussion

Modification of surfaces with positively charged SAM is an effective tool for DNA immobilization. The scheme of DNA immobilization on metal surfaces and its coating with PAN is shown in Fig. 1. The first step is a modification of the gold surface with a 4-ATPh layer. The next step (Fig. 1, step II) is the DNA immobilization on such modified surface. Incubation of 20 nM solution of poly(dG)–poly(dC) results in binding of the DNA to the positively charged surface. The subsequent assembly step (Fig. 1, step III) includes binding of anilinium monomers to the DNA modified surface due to electrostatic interactions as verified in previous studies [11–13,20,21]. The last step (Fig. 1, step IV) is the electrochemical oxidation of anilinium monomers which are bounded to the DNA modified surface.

Impedance spectroscopy of the modified Au surfaces enables to monitor the various surface reaction steps. The impedance spectra include a semicircle portion and a linear portion. The semicircle portion at higher frequencies corresponds to the electron-limited process, and the linear part at lower frequencies corresponds to the diffusion-controlled process. The semicircle diameter corresponds to the electron transfer resistance (R_{et}) from electrode surface to solution species [27], which is measured from the impedance spectroscopy and can be translated into the exchange current (I_0). Then the heterogeneous electron rate constant (K_{et}) can be evaluated using Eqs. (1) and (2) where R is the gas constant, T is the temperature, A is the surface area, F is Faraday constant, [S] is the concentration of the redox probe and n is the number of electrons per redox probe molecule.

$$R_{et} = \mathrm{R}T(nFI_0)^{-1} \quad (1)$$

$$I_0 = nFAK_{et}[\mathrm{S}] \quad (2)$$

Fig. 2 shows the Nyquist diagram (Z_{im} *vs.* Z_{re}) for each modification step. Here the electron transfer resistance (R_{et}) of the bare gold surface was $\sim 133\ \Omega$ ($K_{et} = 3.9 \times 10^{-4}\ \mathrm{cm\ s^{-1}}$). Following the surface modification with 4-ATPh (step I in Fig. 1) this value decreased to $\sim 123\ \Omega$ ($K_{et} = 4.2 \times 10^{-4}\ \mathrm{cm\ s^{-1}}$), and subsequent to the DNA immobilization (step II in Fig. 1) it increased up to 357 Ω ($K_{et} = 1.4 \times 10^{-4}\ \mathrm{cm\ s^{-1}}$).

Surface modification by amine-terminated monolayers is a useful tool for negatively charged species immobilizations [27,28]. This is due to the partial protonation of the terminal amine groups and the creation of positively charged surfaces [29]. Electrostatic interaction between the positively charged anilinium groups of the 4-ATPh and the negatively charged $[\mathrm{Fe(CN)_6}]^{-3/-4}$ accelerates electronic communication between the redox probe and the metal surface and results in R_{et} reduction. On the contrary, the increase of R_{et} as a result of the DNA binding to the electrode is due to the repulsion between the negatively charged DNA and $[\mathrm{Fe(CN)_6}]^{-3/-4}$ as suggested also in the previous studies [27,30].

The double layer capacitance (C_{dl}) can be calculated from the impedance spectra by Eq. (3)

$$\omega_0 = (C_{dl}R_{et})^{-1} \quad (3)$$

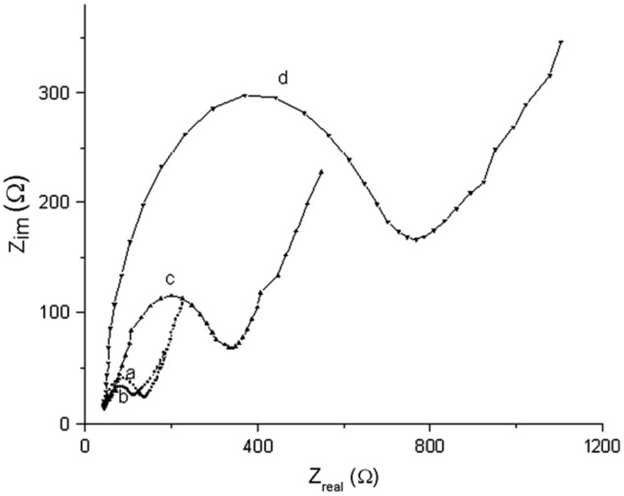

Fig. 2. Nyquist diagram (Z_{im} *vs.* Z_{real}) for the AC impedance measurement in 5 mM $\mathrm{K_3Fe(CN)_6}$ and 0.05 M KCl of: (a) bare Au electrode; (b) the electrode after modification with 4-ATPh; (c) the electrode after DNA immobilization; and (d) the electrode after electropolymerization.

where ω_0 is the characteristic frequency corresponding the frequency of the imaginary part's maximum value of the semicircle in the Nyquist diagram and C_{dl} depends on the dielectric permittivity introduced into the double layer charged molecules and for the less polar molecules the capacitance should be smaller [31]. The C_{dl} value for the bare gold, which was calculated to be 6.3 $\mu\mathrm{F/cm^2}$, increases to 6.9 $\mu\mathrm{F/cm^2}$ following the assembly of 4-ATPh on gold. This rise is attributed to the enhanced surface polarity due to the assembly of quaternary amine-containing monolayer. Upon DNA surface immobilization the C_{dl} value decreases to 3.5 $\mu\mathrm{F/cm^2}$. Such decrease in the capacitance is due to the quaternary amines' neutralization and the overall reduction in surface polarity.

Thickness comparison of the different deposited layers was performed by AFM in contact mode. A 300-nm^2 area was scratched and compared with a non-scratched area of the deposited 4-ATPh, DNA and PAN layers. The scratching of the modified surface with the AFM tip in contact mode shows that the thickness of the deposited 4-ATPh layer was about 5–10 Å. The layer thickness of the 4-ATPh was estimated from the height difference between the bottom of the scratched area and the top of the near by surface of the non-scratched area. The same scratching procedure was repeated after DNA deposition. The layer thickness variation suggests that the DNA anchoring layer is a monolayer with bilayer-containing domains (see Supplementary data). The DNA immobilization resulted in an increase of the layer thickness to about 20 Å as estimated from the height difference between the scratched and non-scratched areas.

The DNA modified surface was incubated with anilinium ions. The incubation resulted in spontaneous bounding of the anilinium ions along the DNA macromolecules. The subsequent electrochemical oxidation resulted in polymerization of the anilinium monomers, causing the formation of PAN layer on DNA and an increase of the surface layer thickness. The final thickness of all the layers, the 4-ATPh and the PAN coated DNA was measured by AFM, by scratching the modified surface as done for the two former deposited layers of 4-ATPh and DNA separately, and found to be 45 Å. We note here that the AFM data cannot provide an accurate estimation of the increased thickness, due to resolution limits and additional forces involved. It can, however, indicate the thickness changes in a comparative way and point to the fact that the thickness indeed increased.

The electrochemical polymerization (step IV in Fig. 1) was carried out using cyclic voltammetry, by cycling the voltage between 0 and 1 V with a scan rate of 50 mV/s, in anilinium-free buffered electrolyte solution. Thus, the monomer's oxidation peak can be attributed to the electrostatically bounded anilinium ions on DNA modified surface (Fig. 1, step III). The electrochemical oxidation of the anilinium monomers and PAN formation are demonstrated in Fig. 3. The two peaks around 0.66 V and around 0.84 V correspond to the electrochemical oxidation of 4-ATPh and anilinium monomers, respectively [12,24]. Subsequent to the oxidation of 4-ATPh in the first cycle, no redox peaks are observed in the following cycles for this molecule. However, the anilinium's oxidation peak decreases with increasing the number of oxidative cycles, while new peaks around 0.34 V (oxidation) and 0.31 V (reduction), which are indicative of the PAN formation [12], grow gradually (Fig. 3, inset).

In order to prove that the electrochemical oxidation indeed resulted in PAN formation on this surface, we performed the following experiment. The sample was withdrawn from the solution, rinsed with water and immersed into a fresh assay solution and voltammograms were again recorded with variable scan rates, between 50 and 300 mV/s (Fig. 4). As seen in Fig. 4 even the first cycle of the electrochemical oxidation measured with this surface is characterized by the peaks around 0.30 V proving that PAN is indeed surface bound. Both the anodic and cathodic peaks measured

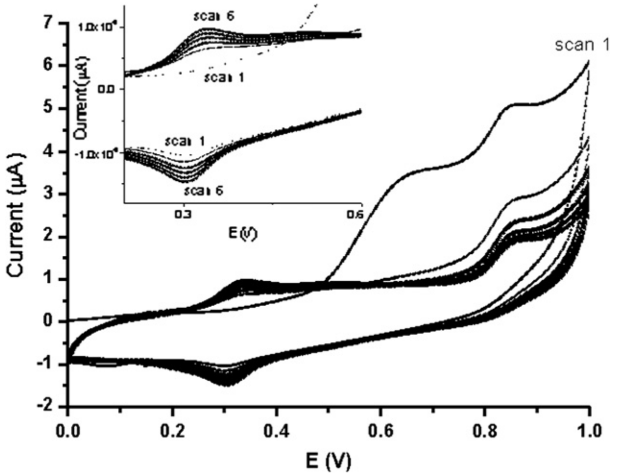

Fig. 3. CV diagram for PAN formation on poly(dG)–poly(dC) (step IV in Fig. 1) measured between 0 and 1 V *vs.* Ag/AgCl at scan rate of 50 mV/s in 50 mM sodium acetate buffer (pH 4) with 4-ATPh modified Au electrodes.

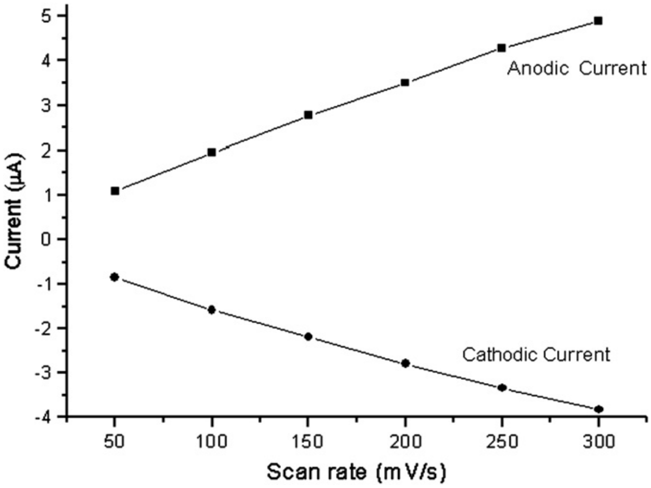

Fig. 5. I_p–scan rate dependence of PAN layer on poly(dG)–poly(dC) DNA.

on this surface are stable, reversible and characterized by higher currents at faster scan rates. I_P–υ experiments were carried out in the range of 50–300 mV/s (Fig. 5). The linear dependence of the current on scan rate proves that the electron mediator is bound to the surface and that the slope of the I_P–υ can be used to calculate PAN surface coverage according to Eq. (4) [12,32] at 298 K

$$I_p = \left(9.39\times10^5\right)n^2\upsilon A\Gamma_0 \tag{4}$$

which can be used for reversible reactions which are present in our case where I_p is peak current, n number of electrons, υ is scan rate, A electrode area, Γ_o is surface coverage which is calculated to be 1.3×10^{-10} mol/cm^2.

The electrochemical oxidation of the anilinium ions is also evident from the impedance spectroscopy data (Fig. 2d); the polymerization leads to a strong increase of R_{et} to 700 Ω; ($K_{et} = 0.7\times10^{-4}$ cm s^{-1}). This increase of R_{et} could be due to electrochemical oxidation of 4-ATPh layer and its integration with PAN [23] which is yielding coverage of the gold surface with polyaniline layer and causing a steric barrier for electron transfer from the gold surface to the solution's redox active species. Consequently causing increase in K_{et} and also decrease in C_{dl} to 2.1 μF/cm^2 showing a clear change in the surface structure due to the polymerization.

PAN formation was also investigated by means of absorption spectroscopy. UV–vis spectroscopy measurements were performed on a semi-transparent thin gold layer coated glass [33]. The differential UV–vis spectra of the coated surface before and after the electrochemical polymerization are shown in Fig. 6. The band around 350 nm is attributed to the absorption band of 4-ATPh molecules. Due to the formation of the π–π* bands of the PAN past polymerization an increase of the 350 nm peak intensity is observed and an additional band around 700 nm appears. The latter is attributed to the π–π* and to the polaron state of the PAN [12]. This peak strongly indicates again the formation of PAN on the DNA-bound surface.

Single molecules are of current interest in the nanosciences due to the growing quest for miniaturizing electronic devices [34,35]. In order to study the wrapping of single molecules DNA with PAN, low concentration of DNA of 1 nM was used to isolate single DNA molecules on the 4-ATPh modified surface. The formation of PAN layer on single DNA macromolecules was followed by AFM imaging. Although calibration of the height differences measured by AFM is inaccurate, the investigation of several samples and a statistical study demonstrate clear height differences between the bare and coated DNA. Fig. 7a shows an AFM image of isolated single DNA macromolecules on 4-ATPh modified gold surface. The height of the DNA macromolecules is approximately 8 Å, as seen in the inset.

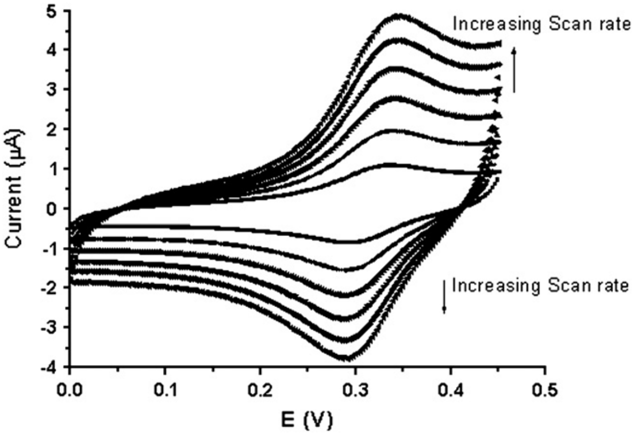

Fig. 4. CV diagram for the 4-ATPh modified Au electrodes with immobilized PAN coated poly(dG)–poly(dC) DNA (product of step IV in Fig. 1) in 50 mM sodium acetate buffer at pH 4 measured with changing scan rate between 50 and 300 mV/s.

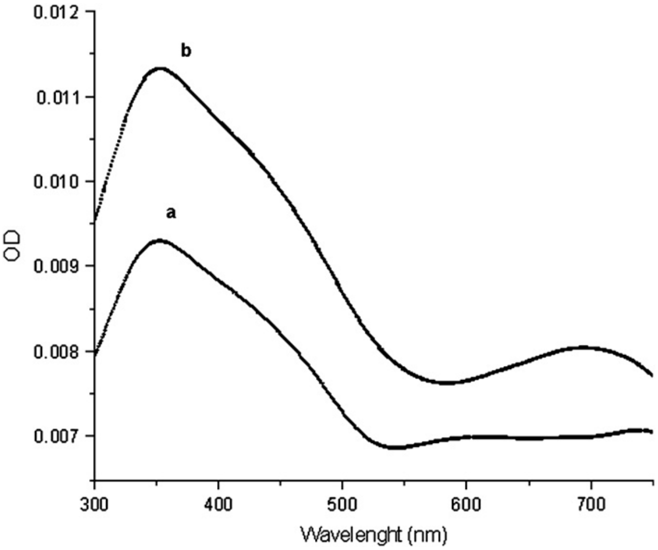

Fig. 6. UV–vis differential spectrum (a) before polymerization (step III in Fig. 1) and (b) after polymerization (step IV in Fig. 1).

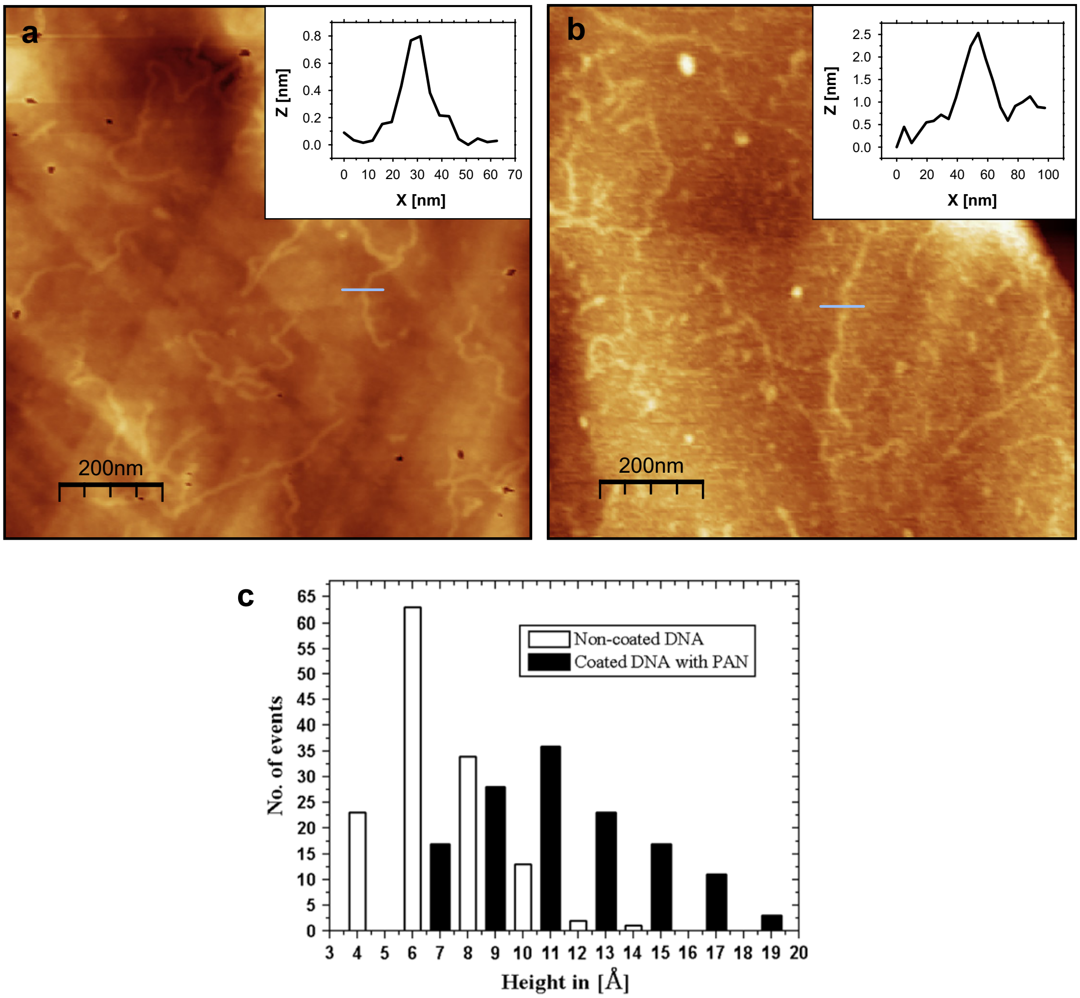

Fig. 7. AFM imaging of: (a) single molecules of poly(dG)–poly(dC); (b) single poly(dG)–poly(dC) coated with PAN. (c) The height distribution of poly(dG)–poly(dC) molecules before and after coating with PAN statistics was done on ∼300 molecules.

Incubation of the surface-bound DNA with anilinium ions followed by electrochemical oxidation of the anilinium monomers resulted in an increase of the macromolecules' height to about 16 Å, as seen in Fig. 7b. The measured height fits nicely the expected thickness of single PAN coated DNA macromolecule-based nanowires. It is also noteworthy that electrochemical polymerization data observed for the single molecules are similar with that of DNA monolayers. This observation supports the adsorption of anilinium ions also to DNA free regions on the surface and oxidation of 4-ATPh monolayer together with adsorbed anilinium ions yielding a PAN layer on the gold surface. To that end, such evidence can be seen also by the AFM results, before the polymerization the gold surface can be analyzed cleanly while following the polymerization gold surface seems covered with a layer. The statistical height distributions of DNA macromolecules before and after electrochemical polymerization are shown in Fig. 7c. The distribution shows that the peak height of non-coated DNA molecules is 6 Å while after PAN coating it is 11 Å, indicating that the height of PAN layer is ∼5 Å which fits well with our previous studies [12]. The coating is not homogeneous, as seen from the height distribution width after the coating.

4. Conclusion

We demonstrated that modification of a gold substrate with 4-ATPh results in efficient binding of DNA monolayer and single DNA molecules can be isolated on the surface. The surface-bound DNA was used as a template for attachment and alignment of anilinium monomers. A new method for *electrochemical oxidation* of anilinium monomers aligned on poly(dG)–poly(dC) resulted in PAN formation along the DNA. Formation of PAN layer on single DNA macromolecules might be useful as conductive nanowires.

Acknowledgements

This work was supported by the EC through contracts IST-2001-38951 ("DNA-Based Nanowires") and FP6-029192 ("DNA-Based Nanodevices"). Y.B. thanks the Israel Ministry of Absorption for the graduate scholarship.

Appendix. Supplementary data

Supplementary data associated with this article can be found in the online version, at doi:10.1016/j.polymer.2008.03.014.

References

[1] He H, Zhu J, Tao NJ, Nagahara LA, Amlani I, Tsui R. Journal of the American Chemical Society 2001;123:7730.
[2] Holtz JH, Asher SA. Nature 1997;389:829.
[3] Pernout JM, Reynolds JR. Journal of Physical Chemistry B 2000;104:4080.
[4] Chiang JC, MacDiarmid AG. Synthetic Metals 1986;13:193.
[5] Paul EW, Rico AJ, Wrighton MS. Journal of Physical Chemistry 1985;89:1441.

[6] Talaie A, Lee JY, Lee YK, Jang J, Romagnoli JA, Taguchi T, et al. Thin Solid Films 2000;363:163.
[7] Kitani A, Yano J, Sasaki K. Journal of Electroanalytical Chemistry 1986;209: 227.
[8] Lee CY, Song HG, Jang KS, Epstein AJ, Joo J. Synthetic Metals 1999;102:1346.
[9] Fou AC, Rubner MF. Macromolecules 1995;28:7115.
[10] Clark SL, Montague MF, Hammond PT. Macromolecules 1997;30:7237.
[11] Turyan I, Mandler D. Journal of the American Chemical Society 1998;120: 10733.
[12] Sfez R, De-Zong L, Turyan I, Mandler D, Yitzchaik S. Langmuir 2001;17:2556.
[13] Sfez R, Peor N, Cohen SR, Cohen H, Yitzchaik S. Journal of Materials Chemistry 2006;16:4044.
[14] Seeman NC. Accounts of Chemical Research 1997;30:357.
[15] Seeman NC. Nature 2003;421:427.
[16] Coffer JL, Bigham SR, Pinizzotto RF, Yang H. Nanotechnology 1992;3:69.
[17] Braun E, Eichen Y, Sivan U, Ben-Yoseph G. Nature 1998;391:775.
[18] Patolsky F, Weizmann Y, Lioubashevski O, Willner I. Angewandte Chemie International Edition 2002;41:2323.
[19] Richter J, Seidel R, Kirsch R, Mertig M, Pompe W, Plaschke J, et al. Advanced Materials 2000;12:507.
[20] Nickels P, Dittmer WU, Beyer S, Kotthaus JP, Simmel FC. Nanotechnology 2004; 15:1524.
[21] Ma Y, Zhang J, Zhang G, He H. Journal of the American Chemical Society 2004; 126:7097.
[22] Nalwa HS. Handbook of organic conductive molecules and polymers. USA: John Wiley and Sons; 1997.
[23] Raj RC, Kitamura F, Ohsaka T. Langmuir 2001;17:7378.
[24] Xie QJ, Gu XL, Zhang YY, Xu MC, Ma M. Chinese Chemical Letters 1999;10:63.
[25] Shapir E, Cohen H, Sapir T, Borovok N, Kotlyar AB, Porath D. Journal of Physical Chemistry B 2006;110:4430.
[26] Horcas I, Fernandez R, Rodriguez JMG, Colchero J, Herrero JG, Baro AM. Review of Scientific Instruments 2007;78:013705.
[27] Xu J, Zhu JJ, Huang Q, Chen HY. Electrochemistry Communications 2001;3:665.
[28] Wang M, Wang L, Wang G, Ji X, Bai Y, Li T, et al. Biosensors and Bioelectronics 2004;19:575.
[29] Ofir Y, Zenou N, Goykhman I, Yitzchaik S. Journal of Physical Chemistry B 2006;110:8002.
[30] Kenneth RB, Audrey PF, Micahel JN. Journal of the American Chemical Society 1996;118:1154.
[31] Willner I, Katz E. Electroanalysis 2003;15:913.
[32] Bard AJ, Faulkner LR. Electrochemical methods fundamentals and applications. USA: John Wiley and Sons; 2001.
[33] Wanunu M, Vaskevich A, Rubinstein I. Journal of the American Chemical Society 2004;126:5564.
[34] Bocharova V, Kiriy A, Vinzelberg H, Monch I, Stamm M. Angewandte Chemie International Edition 2005;44:6391.
[35] Dong L, Hollis T, Fishwick S, Connolly BA, Wright NG, Horrocks BR, et al. Chemistry European Journal 2007;13:822.